References

Gent, P. R., K. O'Neill, and M. A. Cane (1983) A model of the semiannual oscillation in the equatorial Indian Ocean. *Journal of Physical Oceanography, 13*, 2148-2160.

McCreary, J. P. (1984) Equatorial beams. *Journal of Marine Research, 42*, 395-430.

Mied, R. P. and J. P. Dugan (1974) Internal gravity wave reflection by a layered density anomaly. *Journal of Physical Oceanography, 4*, 493-498.

Philander, S. G. H. (1978) Forced oceanic waves. *Reviews of Geophysics and Space Physics, 16*, 15-46.

Peter R. Gent
National Center for Atmospheric Research
P. 0. Box 3000
Boulder, CO 80307

James R. Luyten
Woods Hole Oceanographic Institution
Woods, Hole, MA 02543

Another Simulation of the Seasonal Cycle in the Tropical Atlantic Ocean

Interest has focused on the tropical ocean during the last decade because of its interaction with the global atmospheric circulation, a major component of climate dynamics. From 1982 to 1984, the seasonal variability of the tropical Atlantic Ocean has been investigated through the French Ocean and Climate in the tropical Atlantic (FOCAL) and the American Seasonal Equatorial Atlantic (SEQUAL) programs. The Atlantic Ocean is characterized by its small size and the large variability of the overlying winds. Therefore, it constitutes a good place for testing and understanding the physics that produce the tropical ocean seasonal variability. For this purpose, different approaches have been used in the SEQUAL and FOCAL programs: analysis of historical data; a 2-year observation network; and numerical modeling. The work reported here fits into the first and third activities.

Recently, several numerical models have been adapted to the tropical Atlantic Ocean. The first one, from Busalacchi and Picaut (1983), is a linear-reduced gravity model with a realistic coastline, forced with climatological winds. A second linear model with decomposition into vertical modes, assuming a mean vertical density structure, but with a simple shaped basin, is from du Penhoat and Tréguier (1984). It is also forced with climatological wind stresses. They both successfully demonstrate the importance of the wind forcing in the tropical ocean.

We also studied the linear seasonal response in the upper tropical Atlantic Ocean. We will shortly describe the model and define the parameters used. (The numerical scheme is described in Delecluse (1984) and Levy (1984).)

The model computes the response of the tropical Atlantic Ocean to climatological winds through a single baroclinic mode. The horizontal equations are equivalent to the shallow-water equations where the parameters are the equivalent depth, he, and the phase velocity, c. As shown in the literature and confirmed by our results, this type of model is able to simulate quite well the seasonal variations of the thermocline depth. However, the model currents are less satisfactory. This model is used to investigate the adjustment of the upper ocean to changing wind stresses.

The choice of the baroclinic mode determines the effective amplitude of the wind stress, which is multiplied by the coupling coefficient, and the speed of the oceanic adjustment. We have chosen he = 48 cm and c = 2.17 m s^{-1}, which correspond to the first mode obtained from a vertical density profile typical of tropical Atlantic Ocean (du Penhoat and Tréguier, 1984). This mode represents a large part of their model dynamic height variability. The correct results would be obtained by combining all vertical modes. Our results will show that a large part of the signal is represented by this mode and that the many features of the solution are in good agreement with historical data and other models of the same kind.

The shallow-water equations are discretized on a grid with a variable mesh size, depending upon the area of interest. In longitude, the smallest mesh size (80 km) is near the east and west coasts. It grows up to 111 km in the center of the basin. In latitude, the smallest mesh size is about the equator (88 km), which resolves correctly the equatorial radius of deformation, le = 300 km. The coast line has been defined from bathymetric data from the NOAA Geophysical Fluid Dynamics Laboratory. Two types of boundary conditions have been used: on the coastal boundaries, we have imposed no slip conditions and on the oceanic boundaries, we have imposed a wave radiation condition (Orlanski, 1976) allowing incoming energy to cross the boundary. The model is forced by the wind stresses of Hellerman and Rosenstein's (1983) file. The wind stresses reproduce a climatological year, which is represented by monthly averages on a 2° × 2° grid. These wind stresses are linearly interpolated in space on the model grid. In time, they are Fourier-decomposed and the first five harmonics are retained (the annual mean, and the annual, semiannual, 4 month and 3 month periods).

The results presented here concern the depth of the thermocline after a 4 year run. They are compared with dynamic height with respect to 500 db obtained from historical data gathered for the FOCAL experiment (the data and their processing are described in Delcroix, 1983; Arnault, 1984; Merle and Arnault, 1984). In Figure 1, these fields (computed depth of the thermocline and observed dynamic height) are presented for February and August.

August corresponds to the tropical Atlantic summer-fall season. Dynamic sea-surface topography presents strongly

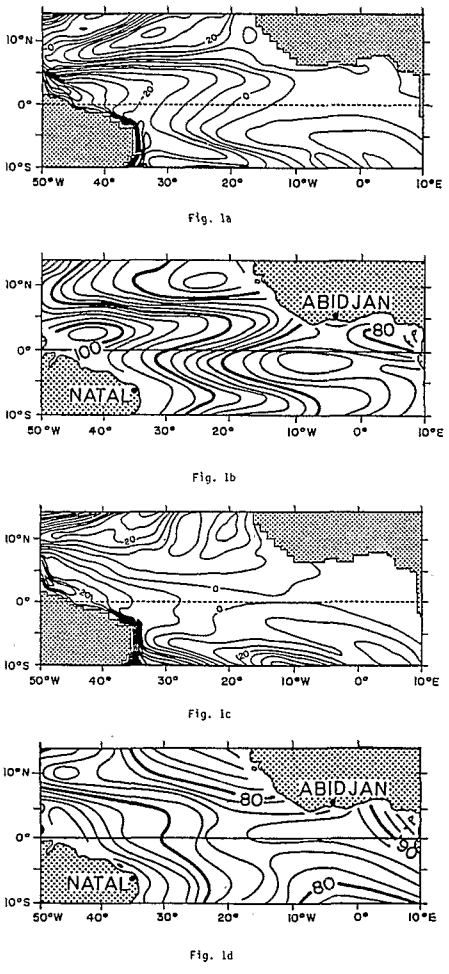

FIGURE 1 (*Arnault et al.*)
Depth of the thermocline computed by the model (a and c) (in meters) and dynamic height relative to 500 db (in dynamic centimeters) issued from data (b and d) for August and February.

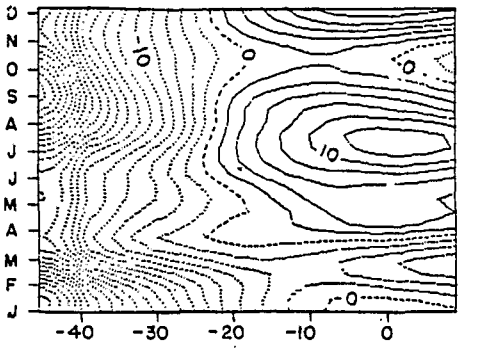

Fig. 2a

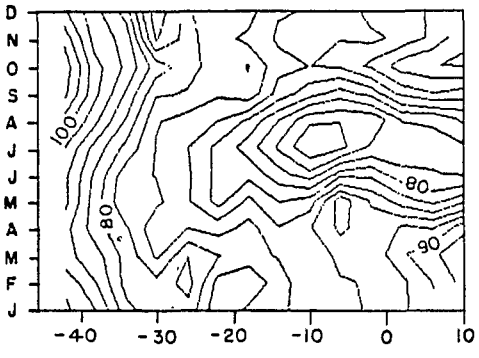

Fig. 2b

FIGURE 2 (*Arnault et al.*)
Monthly variations along the equator of the computed depth (in meters) of the (a) thermocline and (b) dynamic height (in dynamic centimeters).

contrasted zonal ridges and troughs. These features are well simulated by the model, a ridge for the dynamic height being equivalent to a trough in the depth of the thermocline. A first ridge extends from 7°N in the west to 10°N in the east of the basin. A trough at about 2°-3°N is bordering the southern limit of the North Equatorial Countercurrent. The geostrophic zonal component of this current is proportional to the meridional gradient between the 10°N high and 2°-3°N low. Further south, another ridge appears at 3°S, incurving southward upon reaching the African coast. This rather south location disagrees slightly with data. We can also notice in the model results a strong signal along the Brazilian coast. This signal does not appear in the data because of the distribution, but direct measurements during the SEQUAL experiment have confirmed the existence of such coastal eddies (Bruce and Kerling, 1984). Superimposed on these meridional structures is an important east-west slope; the thermocline is deeper in the west than in the east of the basin (Gulf of Guinea).

This summer-fall situation is far different from that of winter-spring, as revealed by the February pictures. Both in the observed dynamic height and in the computed depth of the thermocline, the structures have almost disappeared. The sea-surface topography is rather flat, especially along the equator where the zonal gradient is considerably reduced in the western part.

This annual cycle is even more evident in Figure 2, which shows the seasonal variation along the equator of both the computed depth of the thermocline and the observed dynamic height. In the western part of the basin, both the dynamic height and depth of the thermocline reach an extreme value in April-May. The thermocline is then shallower. It deepens suddenly from June to September-October, when the deepest interface is observed (highest dynamic height). There is also a westward displacement of this maximum from 30°W in July to 40°W in October. This fluctuating motion of the thermocline in the western part of the basin is directly related to the zonal wind stress. The zonally averaged pressure gradient in the observed dynamic height balances the mean zonal wind stress, a balance also reproduced in the model. As shown by Figure 3a, phase and amplitude of variation are similar in the observations and the simulations.

The eastern part of the basin has a different type of variability. Three extrema are present in the model simulations (Figure 2). The interface is deepest in November and February; it is shallowest in July. This annual signal is also close to the observed dynamic height signal, except for the large reversal of the slope, which occurs between 0° and 4°W in the data, but not so clearly in the model simulations. In fact, the model results do not reproduce the disagreement existing between the observed mean zonal wind stress and pressure gradient in the Gulf of Guinea (Figure 3b). The mean zonal pressure gradient computed by the model along the equator still balances the mean zonal wind stress in the eastern part of the basin even though the zonal pressure gradient issued from dynamic height presents a far larger amplitude of variation.

However, these preliminary results, as a whole, indicate a broad agreement with the observed seasonal cycle of dynamic height. They confirm the ability of such a model to simulate the seasonal variations of the depth of the thermocline. The agreement signifies that, to a large part, the variability of the dynamic height is due to an adjustment to varying wind stresses. This is particularly true in the western Atlantic Ocean.

As mentioned in the introduction, two other linear models forced by climatological wind have been used to simulate the tropical Atlantic Ocean. Even when all these models successfully demonstrate the importance of the wind forcing in the tropical oceans, they present slight differences, almost as large as the differences in climatological dynamic height. A qualitative comparison among the results of these models and historical data has pointed out the probable influence of particularities, such as choice of a baroclinic mode in regard to others and boundary conditions. This analysis and its results will be

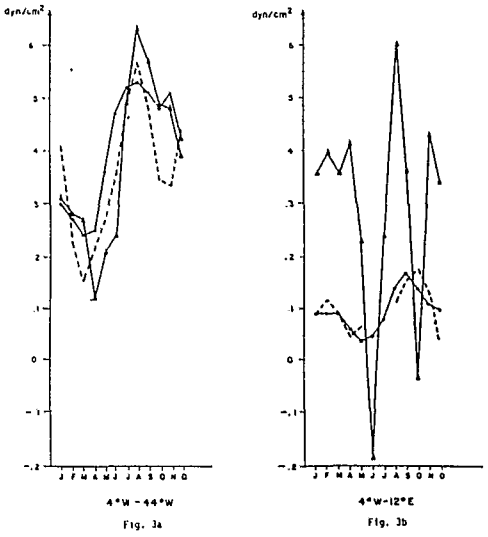

FIGURE 3 (*Arnault et al.*)
Seasonal variations along the equator of the mean zonal wind stress (solid line and points), of the zonal pressure gradient issued from dynamic height (solid line and triangles) or computed by the model (dashed line) for the (a) western part or (b) eastern part of the basin. (Units are dynes per square centimeter.)

presented in a forthcoming paper, because there is a need to investigate the differences between them so that we may progress with the modeling of the equatorial Atlantic Ocean.

References

Arnault, S. (1984) Variation saisonniere de la topographie dynamique et de la circulation superficielle de l'océan Atlantique tropical. Thèse de doctorat de 3 cycle, Université Pierre et Marie Curie, Paris.

Bruce, J.G. and J.L. Kerling (1984). Near equatorial eddies in the North Atlantic. *Geophysical Research Letters, 11,* 779-782.

Buslacchi, A. J. and J. Picaut (1983) Seasonal variability from a model of the tropical Atlantic Ocean. *Journal of Physical Oceanography, 13,* 1564-1588.

Delcroix, T. (1983) Variations saisonnieres de la profondeur de la thermocline dans l'océan Atlantique tropical: Role des alizés. Thèse de doctorat de 3 cycle, Université Pierre et Marie Curie, Paris.

Delecluse, P. (1984) Dynamique océanique équatoriale: Influence des frontieres Est et Ouest. Thèse de doctorat d'état, Université Pierre et Marie Curie, Paris.

du Penhoat, Y. and A-M. Tréguier (1984) The seasonal linear response of the tropical Atlantic Ocean. *Journal of Physical Oceanography,* accepted.

Hellerman, S. and M. Rosenstein (1983)

Normal monthly wind stress over the world ocean with error estimates. *Journal of Physical Oceanography, 13,* 1093-1104.
Levy, C. (1984) Modélisation numérique du cycle saisonnier de l'océan Atlantique tropical: Role des fronts de vents. Thèse de doctorat de 3 cycle, Université Pierre and Marie Curie, Paris.
Merle, J. and S. Arnault (1984) Seasonal variability of the surface dynamic topography in the tropical Atlantic Ocean. *Journal of Marine Research,* accepted.
Orlanski, I. (1976) A simple boundary condition for unbounded hyperbolic flow. *Journal of Computational Physics, 21,* 251-269.

5
Sabine Arnault
Pascale Delecluse
Claire Levy
Laboratoire d'Océanographie-Physique
Muséum National d'Histoire Naturelle
43-45 Rue Cuvier
75 231 Paris Cedex 05
France

Unusual Amounts of Very Saline Subsurface Water in the Eastern Gulf of Guinea in May 1984

In this note, we document the presence in May 1984 of a large subsurface pool of anomalously salty waters in the eastern equatorial Gulf of Guinea, and we offer a partial explanation that agrees with some existing hypotheses about the hydrography and the circulation in that region. We suggest the following scenario: the high salinity originates in the west and is advected eastward by the Equatorial Undercurrent (EUC). Equatorial upwelling and subsequent vertical mixing west of 0°E breaks the originally eastward directed salt tongue and produces an inversion of the zonal salt gradient. The unusually high 1984 values of salinity east of 0°E were caused by an anomalously low loss of salt by the EUC core during its eastward course, rather than by a positive salt anomaly at the western source of the current.

The pattern of circulation and of seasonal variations of water properties that we postulate is a synthesis of the work of Hisard and Morliere (1973), Hisard et al. (1975), Wauthy (1977), Voituriez (1983) and others referenced within these papers. In this scheme, the Atlantic EUC reaches the easternmost Gulf of Guinea where its core splits into two branches: one branch spreads northward toward the Bight of Biafra, the other turns southeastward along the coast of Gabon. This picture is based on the assumption that the EUC is the sole source for the salty oxygen-rich (> 4 ml l^{-1}) water observed below the surface in the eastern Gulf of Guinea. Another source of high salinity could be subtropical water advected northwestward from the South Atlantic by the Benguela Current. But this source has been ruled out on the grounds that such water does not reach low enough latitudes, that it remains at the surface and that it has too low an oxygen content (Wauthy, 1977). Eastward, and then poleward, tongues of subsurface salt and oxygen maxima have indeed been traced from the west (Figure 1). Instantaneous Eulerian current measurements are not very useful, because speeds in the region are weak (< 30 cm s^{-1}) and highly variable. In particular, no information is available about the seasonal variations of horizontal transports east of 0°E.

The use of the "core-layer" method, which allows tracing tongues of property extrema, is justified only for nearly conservative tracers. It applies to our case only as long as the EUC remains shielded from external influences; that is, as long as loss of properties along the EUC path occurs simply through slow lateral and vertical diffusion. From roughly November to April each year, the relatively cold salty EUC in the Gulf of Guinea is imbedded in the thermocline below a surface layer of warm fresher water, and the use of tracing techniques is probably reasonable. However, from about June to September, the stratification is reduced as upwelling occurs at the equator and along the coast of southwestern Africa. There is an enhanced loss of properties by the upper layers of the EUC as heat, salt, and oxygen are advected upward. Mixing with overlying warmer and less saline water occurs, and oxygen starts to be depleted by biological consumption. Meanwhile, the lower layers of the EUC receive from below, or from the sides, an influx of water that is poorer in salt and oxygen. Horizontal maps of subsurface property extrema during the upwelling season can, therefore, become misleading.

Two sets of older measurements illustrate the vertical transfer of properties just described. First, at 4°W, during the summer of 1978, the salt content of the eastward flowing EUC was observed to

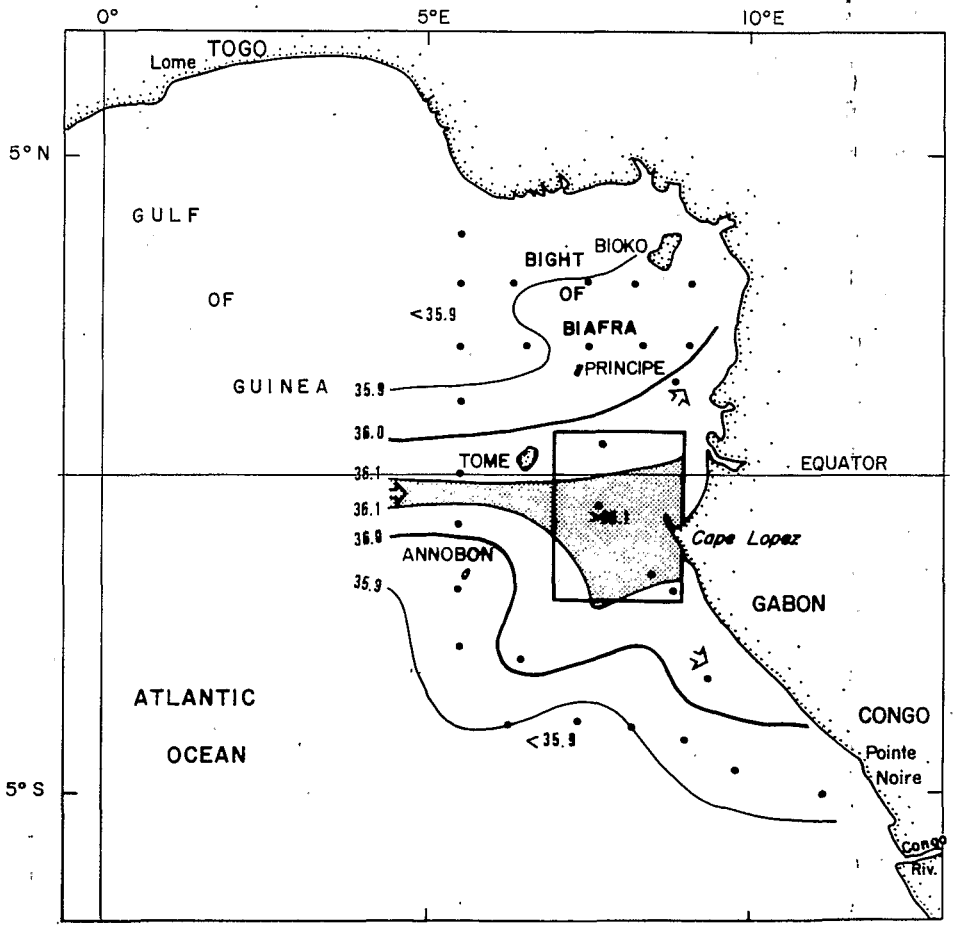

FIGURE 1 (*Piton and Wacongne*)
Horizontal distribution of the equatorial subsurface salinity maximum in the eastern part of the Gulf of Guinea (BIAFRA experiment, 8-23 January 1980). The box indicates the heavily sampled region refered to in the text and in Figure 2. The location of the data points is shown.